Desalination and Water Treatment
www.deswater.com

doi: 10.1080/19443994.2015.1101020

57 (2016) 19391–19401
September

Taylor & Francis
Taylor & Francis Group

Removal of hazardous azocoumarin dye from aqueous solutions using activated carbon prepared from rice straw

Adel Z. El-Sonbati[a], Ashraf A. El-Bindary[a,*], Khaled S. Mohamed[b], Ahmad A. Al-Sarawy[c], Mansour A. Farid[a]

[a]*Faculty of Science, Department of Chemistry, University of Damietta, Damietta 34517, Egypt, Tel. +2 01060081581; email: elsonbatisch@yahoo.com (A.Z. El-Sonbati), Tel. +2 01114266996; email: abindary@yahoo.com (A.A. El-Bindary), Tel. +2 01006167024; email: mansourmansour2005@yahoo.com (M.A. Farid)*
[b]*Engineering Chemistry Department, Higher Institute for Engineering and Technology, Damietta, Egypt, Tel. +2 01222878456; email: khaled_samirm@yahoo.com*
[c]*Faculty of Engineering, Department of Mathematical and Physical Engineering, University of Mansoura, Mansoura, Egypt, Tel. +2 01060678905; email: alsarawy2000@yahoo.com*

Received 29 January 2015; Accepted 22 September 2015

ABSTRACT

Activated carbon made from rice straw (ACRS) was tested as a low-cost adsorbent for the removal of hazardous azocoumarin dye from aqueous solution in batch adsorption procedure. The effect of different variables in the batch method as a function of solution pH, contact time, concentration of adsorbate, adsorbent dosage, and temperature were investigated and optimal experimental conditions were ascertained. More than 85% removal efficiency was obtained within 65 min at adsorbent dose of 0.5 g for initial dye concentration of 100 mg L^{-1} at pH 3. The Brunauer–Emmett–Teller surface area and Barrett–Joyner–Halenda pore volume were calculated and found to be 67.4 $m^2 g^{-1}$ and 0.134 $cm^3 g^{-1}$, respectively. The point of zero charge (pH_{PZC}) of ACRS was determined and found to be 7. The experimental equilibrium data were tested by the isotherm models namely, Langmuir and Freundlich adsorption and the isotherm constants were determined. The results revealed that Freundlich isotherm fit the experimental results well. The kinetic data obtained with different initial concentration and temperature were analyzed using a pseudo-first-order and pseudo-second-order equations. The pseudo-second-order sorption kinetics was the best model and indicates that physorption controls the process. Thermodynamic parameters, such as Gibbs free energy, enthalpy, and entropy of adsorption of the dye-rice straw fly ash systems were evaluated and it was found that the reaction was spontaneous and exothermic in nature.

Keywords: Adsorption; Rice straw; Azocoumarin; Isotherms; Kinetics

1. Introduction

Color is one the major indicators of water pollution that reduces photosynthetic activity by preventing proper sunlight penetration [1]. Effluent treatment process for dye-containing effluents from textile, paper, and tanneries industries are currently capable of removing about only half of the dyes lost in residual liquors [2]. These dyes could be degraded to produce carcinogens and toxic products [3]. Therefore,

---

*Corresponding author.

the treatment of effluent containing such dyes is of great interest due to its harmful impacts on receiving waters [4]. Coumarin derivatives are widely used as additives in food and cosmetics [5], pharmaceuticals, and optical brighteners [6] and fluorescent dyes [7]. Azocoumarin and its derivatives are toxic and carcinogenic in nature. Several methods including adsorption, coagulation, membrane filtration, and advanced oxidation [8–11] have been employed to eliminate dyes from wastewaters. Among them, adsorption has been recognized as a promising technique due to its high efficiency, simplicity of design, ease of operation as well as the wide suitability for diverse types of dyes [12]. Because the dye effluent may cause damage to aquatic biota and human by mutagenic and carcinogenic effects, the removal of dye pollutants from wastewater is of great importance [13]. Various removal methods, in recent years, the search for low-cost adsorbents that have dye-binding capacities has intensified. This has led many workers to search for cheaper alternates such as coal, fly ash, silica gel, wool wastes, agricultural wastes, wood wastes, and clay minerals [14].

In Egypt, rice straw is an easily available agricultural waste material, produced in large quantities as a by-product of rice milling and create potential environmental problems. The waste products which are the main contributors to biomass burning are wheat residue and rice straw. The disposal of rice straw by open-field burning frequently causes serious air pollution, hence new economical technologies for rice straw disposal and utilization must be developed. In order to improve the sorption capacity of these biomaterials, the low-cost agricultural by-products were converted to activated carbon [15]. In continuation to our interest in study on dye adsorption onto low-cost biomaterials [15–18], we synthesize and characterize new hazardous azocoumarin and investigate its adsorption onto a low-cost activated carbon made from rice straw as adsorbent. Physical and chemical characteristics of the adsorbent (ACRS) were evaluated with N_2 adsorption/desorption experiments at 77 K. The influences of adsorption parameters such as initial adsorbate concentration, adsorbent dosage, contact time, solution pH, and temperature on the adsorption performance of azocoumarin were investigated. The kinetic and thermodynamic parameters were also calculated to determine rate constants and adsorption mechanism. The experimental data were fitted into Langmuir and Freundlich equations to determine which isotherm gives the best correlation to experimental data.

2. Materials and methods

2.1. Physical measurements

C, H, and N were determined on Automatic Analyzer CHNS Vario ELIII, Germany. Spectroscopic data of the azocoumarin dye were obtained using the following instruments: FTIR spectrum (KBr discs, 4,000–400 cm^{-1}) by Jasco-4100 spectrophotometer; the ^1H NMR spectrum by Bruker WP 300 MHz using DMSO-d_6 as a solvent containing TMS as the internal standard; mass spectrum by Shimadzu GC–MS-QP2010 Plus instrument. The scanning electron microscopy (SEM) results of the ACRS sample before and after the adsorption processes were obtained using (JEOL-JSM-6510 LV) scanning microscope to observe surface modification. The point of zero charge determination (pH_{PZC}) was determined. UV–vis spectrophotometer (Perkin–Elmer AA800 Model AAS) was employed for absorbance measurements of samples. An Orion 900S2 model digital pH meter and a Gallenkamp Orbital Incubator were used for pH adjustment and shaking, respectively. N_2 adsorption/desorption isotherms on ACRS at 77 K was measured on a Quantachrome Nova Instruments version 10, from which the Brunauer–Emmett–Teller (BET) surface area and Barrett–Joyner–Halenda (BJH) pore volume were calculated.

2.2. Synthesis of azocoumarin dye

3-(4-amino-2-oxo-2H-chromen-3-yl)-5-(2-hydroxy-5-((4-methoxyphenyl)diazenyl) phenyl) furan-2-carbonitrile (Fig. 1) was prepared using a method describes in the literature [18]. A well stirred solution of p-anisidine (1) (0.1 mol) in 2 N hydrochloric acid (125 ml) was cooled in an ice-bath and diazotized with 0.1 N sodium nitrite solution (100 ml). The mixture was stirred at −5˚C for 1 h. The above cold diazonium solution was added dropwise to a well stirred cold solution of (2) in sodium hydroxide solution (5%, 30 ml). The reaction mixture was stirred for 2–3 h until coupling was complete. The solid precipitate was filtered, washed with water, dried and crystallized from absolute ethanol to give (3) with Yield 60%; color: dark brown, solid; mp = >300˚C; FTIR (KBr) (v cm^{-1}): 3,436 (OH), 3,321 (NH_2), 2,198 (CN), and 1,721 (C=O). ^1H NMR (DMSO-d^6): δ 3.84 (s, 3H, CH_3), 4.98 (br, s, 2H, NH_2), 6.84 (s, 1H, C3-H furan), 7.00–8.20 (m, 11H, ArH), 10.21 (s, 1H, OH); MS *m/z* (M+, %) 478, 71.05%. Anal.: Calcd for $C_{27}H_{18}N_4O_5$ (478): C, 67.78; H, 3.79; N, 11.71. Found: C, 67.75; H, 3.81; N, 11.68.

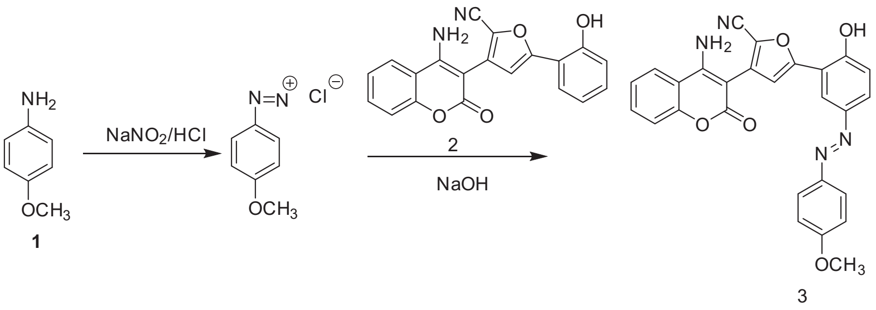

Fig. 1. The structure of azocoumarin dye.

2.3. Preparation of activated carbon made from rice straw

Activated carbon made from rice straw (ACRS) as adsorbent was collected from Tammy Amdid, Dakahlia, Egypt Biogas Factory [18]. The concept is based on the burning of waste rice straw in a special incinerator at the temperature of 1,000–1,200°C. During the burning process, the hydrocarbons are converted to carbon oxides, hydrogen, methane, propane, and other gases. The carbon waste was left to cool down. In our laboratory, the activated carbon made from rice straw (ACRS) was crushed, ground, and sieved through a 200 μm sieve and washed several times with bidistilled water. The adsorbent sample was dried at 120°C for 48 h preserved in the desiccators over anhydrous $CaCl_2$ for further use. IR spectrum of ACRS is of vital importance in understanding the adsorption process and used to determine the vibrational frequencies of ACRS. In ACRS, the FTIR adsorption peaks are: FTIR (KBr) (v cm^{-1}): 3,397 (−SiOH or −OH), 1,585 (C=O), 1,195 (Si–O–Si), and 792 (Si–H) cm^{-1}.

2.4. Determination of point of zero charge

The point of zero charge (pH_{PZC}) was determined by solid addition method [19]. A series of 0.1 M KNO_3 solutions (50 ml each) were prepared and their pH values were adjusted in the range of 1.0–12.0 by addition of 0.1 mol L^{-1} HCl and 0.1 mol L^{-1} NaOH. To each solution, 0.1 g of ACRS was added and the suspensions were shaken manually and the solution was kept for a period of 48 h with intermittent manual shaking. The final pH of the solution was recorded and the difference between initial and final pH (ΔpH) (Y-axis) was plotted against the initial pH (X-axis). The point of this curve yielded pH_{PZC}.

2.5. Adsorption experiments

Batch adsorption studies were carried out by shaking 50 ml conical flasks containing 0.5 g of (ACRS) and 25 mL of dye solutions of desired concentration with adjusted pH on an orbital shaker machine at 200 rpm at 25°C. The solution pH was adjusted with 0.1 mol L^{-1} HCl and 0.1 mol L^{-1} NaOH solutions. At the end of the adsorption period, the supernatant solution was separated by centrifugation at 200 rpm for 10 min. Then the concentration of the residual dye was determined spectrophotometrically by monitoring the absorbance at 503 nm for dye using UV–vis spectrophotometer. Percentage of dye removal (R) was calculated using Eq. (1):

$$R = 100(C_0 - C_t)/C_0 \tag{1}$$

where C_0 (mg L^{-1}) and C_t (mg L^{-1}) are dye concentration initially and at time t, respectively. For adsorption isotherms, dye solutions different concentrations (30–100 mg L^{-1}) were agitated with known amounts of adsorbents until the equilibrium was achieved. Equilibrium adsorption capacity, q_e (mg dye per g adsorbent) was calculated from the following Eq. (2):

$$q_e = V(C_0 - C_t)/W \tag{2}$$

where C_t (mg L^{-1}) is the dye concentration at equilibrium, V (L) is the volume of solution, and W (g) is the weight of adsorbent.

The procedures of kinetic experiments were identical with those of equilibrium tests. At predetermined moments, aqueous samples (5 mL) were taken from the solution, the liquid was separated from the adsorbent by centrifuge at 200 rpm and concentration of dye in solution was determined spectrophotometrically at a wavelength of 503 nm. The amount of dye adsorbed at time t, q_t (mg g^{-1}) was calculated by following Eq. (3):

$$q_t = V(C_0 - C_t)/m \tag{3}$$

where C_0 (mg L^{-1}) is the initial dye concentration, C_t (mg L^{-1}) the dye concentration at any time t, V (L) the volume of the solution, and m (g) is the mass of the adsorbent.

In an adsorption study, it is necessary to fit the equilibrium adsorption data using different adsorption isotherm models and kinetic equations in order to analyze and design an adsorption process. Therefore, different theoretical models are applied to experimental data in order to find a model which adequately predicts kinetic and isotherm data. The validity of the models was evaluated by the coefficient of determination (r^2) [20].

3. Results and discussion

3.1. BET surface area

The BET [21] surface area and BJH pore size of ACRS have been investigated previously [18] using N_2 adsorption/desorption measurements at 77 K. The BET surface area of ACRS was obtained as 67.4 $m^2 g^{-1}$ can supply more surface active sites, leading to an enhancement of adsorption performance. It is suggested that the pore structure of the adsorbent ACRS consists of macropores, mesopores, and micropores. The total pore volume (V_p) at $P/P_o = 0.959$ was obtained as 0.134 $cm^3 g^{-1}$, which indicating that ACRS has a mesoporous structure and makes it easy for azopyrazole dye to penetrate into the mesopores of ACRS.

3.2. SEM analysis

SEM has been a primary tool for characterizing the surface morphology and fundamental physical properties of the adsorbent surface. It is useful for determining the particle shape, porosity, and appropriate size distribution of the adsorbent. Scanning electron micrographs of raw (ACRS) and adsorbed (ACRS) with the dye are shown in Figs. 2 and 3, respectively. It is clear that raw (ACRS) has considerable numbers of pores where there is a good possibility for dyes to be trapped and adsorbed into these pores (Fig. 2). The SEM picture (Fig. 3) of (ACRS) adsorbed with tested dye shows very distinguished dark spots which can be taken as a sign of effective adsorption of azocoumarin molecules in the cavities and pores of this adsorbent.

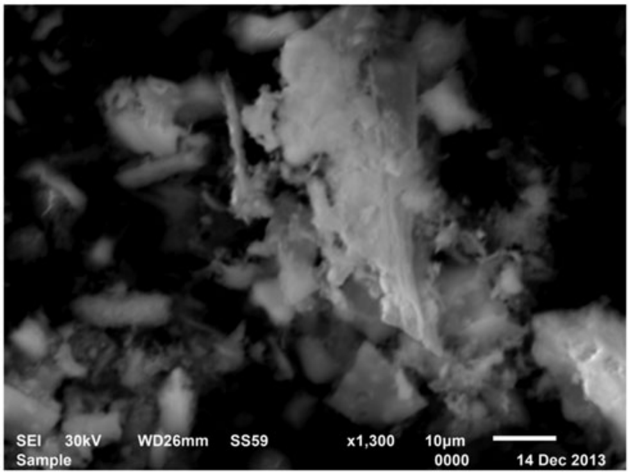

Fig. 2. ACRS before adsorption of azocoumarin dye.

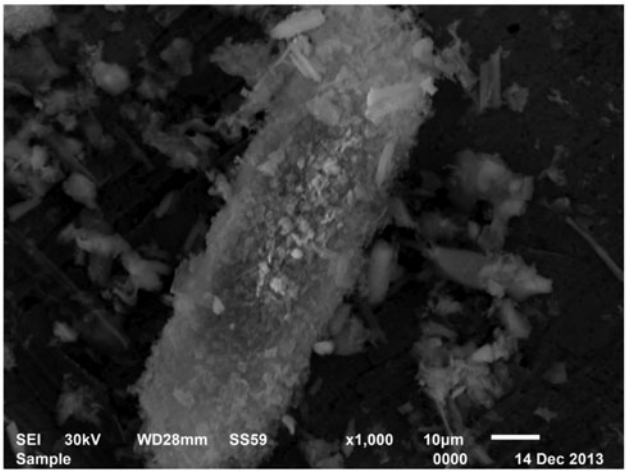

Fig. 3. ACRS after adsorption of azocoumarin dye.

3.3. Determination of point of zero charge (pH_{PZC})

The pH_{PZC} gives very significant information about the type of surface active centers. The pH_{PZC} of ACRS was found to be 7. This shows that below this pH, the ACRS acquires a positive charge due to protonation of functional groups and above this pH, negative charge exists on the surface of ACRS. The adsorption of anionic dyes is favoured at $pH < pH_{PZC}$ where the surface becomes positively charged [22].

3.4. Effect of adsorbate concentrations

The removal of azocoumarin dye by adsorption on the adsorbent (ACRS) was shown to increase with time and attained a maximum value at about 65 min, and thereafter, it remained almost constant (Fig. 4). On changing the initial concentration of dye solution from 30 to 100 mg L^{-1} at 25°C, pH 3 and 0.5 g L^{-1} adsorbent dosage the amount of removed dyes was decreased. It was clear that the removal of the dye

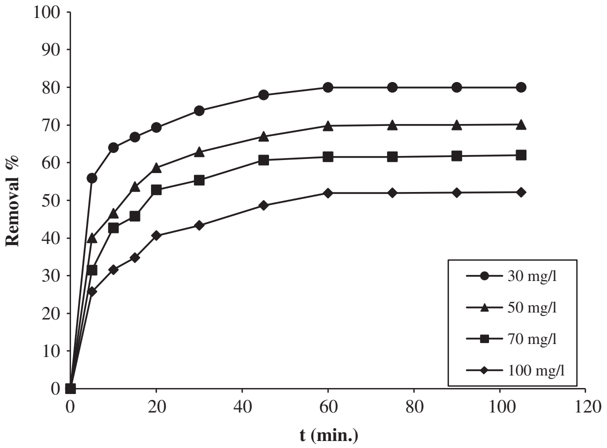

Fig. 4. Effect of initial dye concentration on adsorption of azocoumarin onto ACRS, dosage 0.5 g L^{-1}, pH 3, and 25˚C.

was dependent on the initial concentration of the dye because the decrease in the initial dye concentration increased the amount of dye adsorbed. This is very clear because, for a fixed adsorbent dose, the number of active adsorption sites to accommodate adsorbate ions remains unchanged but with increasing adsorbate concentration, the adsorbate ions to be accommodated increase and hence the percentage of adsorption goes down.

3.5. Effect of adsorbent dosage

The uptake of dye with change in adsorbent dosage (0.1–0.9 g) at adsorbate concentrations of 100 mg L^{-1} at 25˚C and pH 3 is presented at (Fig. 5). Adsorption of dye shows that the uptake of dye per gram of adsorbent increases with increasing adsorbent dosage from 0.1 to 0.9 g. This is because a higher dose of adsorbent, led to increased surface area and more adsorption sites are available causing higher removal of the dye. Further increase in adsorbent dose did not cause any significant increase in % removal of dye. This was due to the concentration of dyes reaching equilibrium status between solid and solution phase.

3.6. Effect of temperature

The results of this study are shown (Fig. 6), which explain the relation between the removal of dye ratio and time at different temperatures (25, 40, 50, and 60˚C) using the (ACRS) adsorbent reveal that the contact time decrease with increasing temperature this might be due to increasing diffusion coefficient with the increase in temperature. In our case, the experimental data obtained at pH 3, adsorbent dosage 0.5 g L^{-1}, and initial concentration of 100 mg L^{-1} show that increase in the adsorption capacity at temperatures from 25 to 60˚C.

3.7. Effect of pH

The removal of the tested dye by activated carbon of rice straw (ACRS) at different pH values was studied at initial concentrations of 100 mg L^{-1} of the dye, 25˚C and 0.5 g L^{-1} adsorbent dosage. The pH value of the solution was an important controlling parameter in the adsorption process. ACRS has proved to be an effective adsorbent for the removal of the dye, which was achieved via adsorption from an aqueous solution

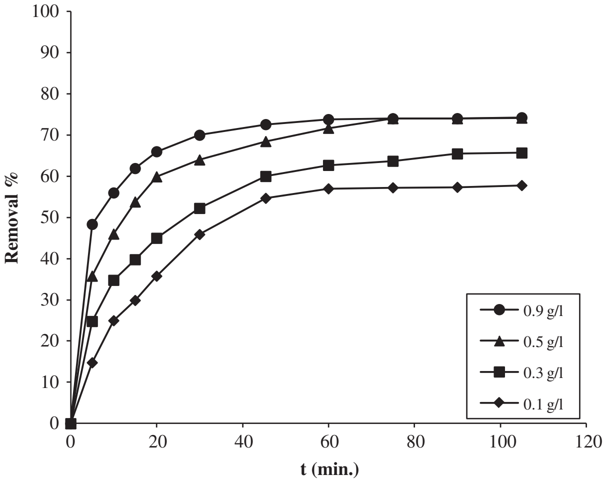

Fig. 5. Effect of ARSC dosage on the adsorption of azocoumarin dye at concentration 100 mg L^{-1}, pH 3, and 25˚C.

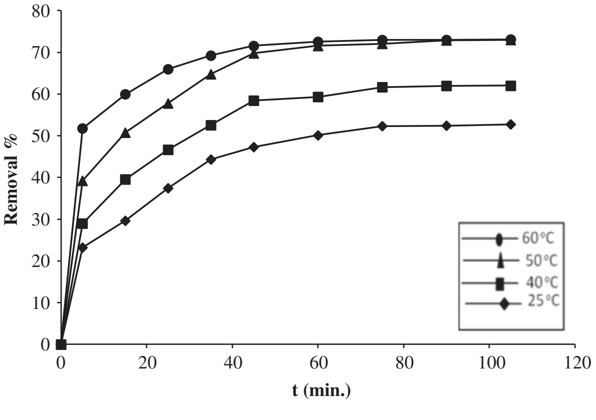

Fig. 6. Effect of temperature on adsorption of azocoumarin dye onto ACRS, dosage 0.5 g L^{-1}, dye concentration 100 mg L^{-1}, and pH 3.

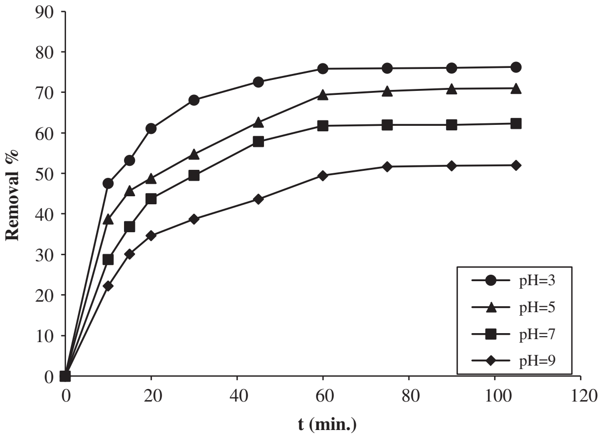

Fig. 7. Effect of pH on adsorption of azocoumarin dye onto ACRS at dosage 0.5 g L^{-1} and temperature 25˚C.

at pH 3 was achieved (Fig. 7). It shows that the adsorption capacity of tested dye onto ACRS increases significantly with decreasing pH. The maximum removals for contact time 65 min were carried out at pH 3.

As the pH of the adsorption system increases, the number of negatively charged sites increases and the number of positively charged sites decreases. A negatively charged surface site on the adsorbent does not favor the adsorption of dye anions, due to the electrostatic repulsion. Also, lower adsorption of tested dye at alkaline pH is due to the presence of excess hydroxyl ions competing with the dye anions for the adsorption sites [23].

3.8. Adsorption isotherms

The main factors that play the key role for the dye-adsorbent interactions are charge and structure of dye, adsorbent surface properties, hydrophobic and hydrophilic nature, hydrogen bonding, electrostatic interaction, steric effect, and van der Waal forces etc. [24]. Equilibrium studies that give the capacity of the adsorbent and adsorbate are described by adsorption isotherms, which is usually the ratio between the quantity adsorbed and that remained in solution at equilibrium at fixed temperature [25]. The equilibrium experimental data for the adsorption of the tested dye on the (ACRS) were compared using two isotherm equations namely, Langmuir and Freundlich.

3.8.1. Langmuir isotherm

The Langmuir adsorption, which is the monolayer adsorption, depends on the assumption that the intermolecular forces decrease rapidly with distance and consequently predicts the existence of monolayer coverage of the adsorbate at the outer surface of the adsorbent. The isotherm equation further assumes that adsorption occurs at specific homogeneous sites within the adsorbent. It then assumed that once a dye molecule occupies a site, no further adsorption can take place at that site. Furthermore, the Langmuir equation is based on the assumption of a structurally homogeneous adsorbent, where all sorption sites are identical and energetically equivalent. Theoretically, the sorbent has a finite capacity for the sorbate. Therefore, a saturation value is reached beyond which no further sorption can occur. The saturated or monolayer capacity can be represented as the known linear form of Langmuir equation [26–29]:

$$C_e/q_e = 1/\left(q_{\max}K_L\right) + C_e/q_{\max} \tag{4}$$

where C_e is the equilibrium dye concentration in the solution (mg L^{-1}), q_e is the equilibrium dye concentration in the adsorbent (mg g^{-1}), $q_{\max}$ is the monolayer capacity of the adsorbent (mg g^{-1}), and K_L is the Langmuir adsorption constant (L mg^{-1}).

Therefore, a plot of C_e/q_e vs. C_e (Fig. 8), gives a straight line of slope $1/q_{\max}$ and the intercept $1/(q_{\max}K_L)$. The Langmuir equation is applicable to homogeneous sorption, where the sorption of each sorbate molecule onto the surface is equal to the sorption activation energy.

3.8.2. Freundlich isotherm

The Freundlich equation [29,30] is an empirical equation employed to describe heterogeneous systems, characterized by the heterogeneity factor $1/n$,

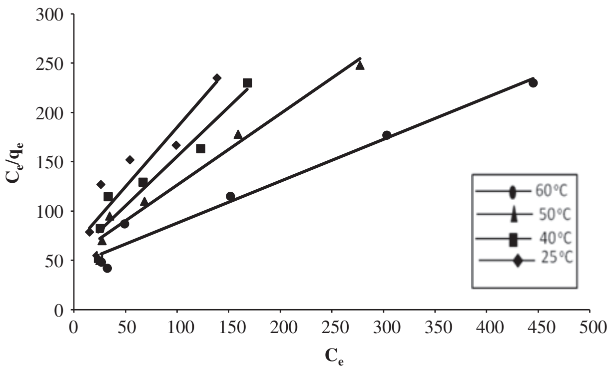

Fig. 8. Langmuir plot for the adsorption of dye azocoumarin dye onto ACRS at different temperatures.

describes reversible adsorption, and is not restricted to the formation of the monolayer:

$$q_e = K_F \cdot C_e^{1/n} \tag{5}$$

where q_e is the equilibrium dye concentration on adsorbent (mg g^{-1}), C_e is the equilibrium dye concentration in solution (mg L^{-1}), K_F is Freundlich constant (mg g^{-1}), and $1/n$ is the heterogeneity factor. A linear form of the Freundlich expression can be obtained by taking logarithms of the equation:

$$\log q_e = \log K_F + 1/n \log C_e \tag{6}$$

Therefore, a plot of log q_e vs. log C_e for the adsorption of tested dye onto ACRS (Fig. 9) was employed to generate the intercept value of K_F and the slope of $1/n$. The correlation coefficients for Langmuir (r_L^2) and for Freundlich (r_F^2) values are compared in Table 1.

One of the Freundlich constants K_F indicates the adsorption capacity of the adsorbent. The other Freundlich constant n is a measure of the deviation from linearity of the adsorption. If a value for n is equal to unity, the adsorption is linear. A value of n was found above unity, this implies that the adsorption process is favorable a physical process [31]. The highest value of n at equilibrium is 1.751 (Table 1), which would seem to suggest that the adsorption is physical, which refers to the adsorption bond which becomes weak [32] and conducted with van der Waals forces.

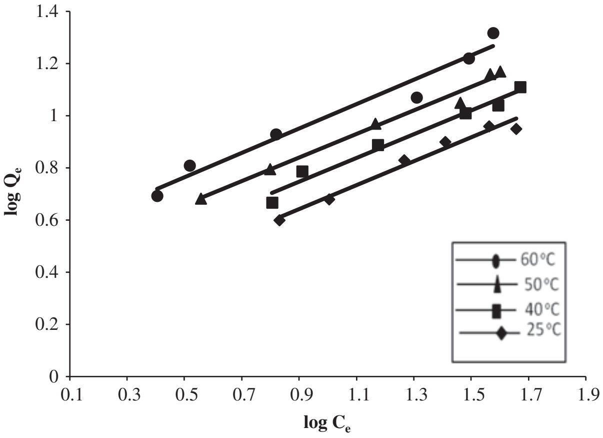

Fig. 9. Freundlich plots for adsorption of azocoumarin dye onto ACRS at different temperatures.

3.9. Adsorption kinetic studies

The study of adsorption kinetics describes the solute uptake rate and evidently this rate controls the residence time of adsorbate uptake at the solid–solution interface. The rate of removal of tested dye by adsorption was rapid initially and then slowed gradually until it attained an equilibrium beyond which there was a significant increase in the rate of removal. The maximum adsorption was observed at 65 min and it is thus fixed as the equilibrium time.

Aiming at evaluating the adsorption kinetics of tested dye onto (ACRS), the pseudo-first-order and pseudo-second-order kinetic models were used to fit the experimental data, according to the below kinetic model equations.

The pseudo-first-order rate expression of Lagergren [33,34] is given as:

$$\log(q_e - q_t) = \log q_e - k_1 t \tag{7}$$

The pseudo-second-order kinetic model [34] is expressed as:

$$t/q_t = 1/k_2 q_2^2 + 1/q_2 t \tag{8}$$

where q_t is the amount of dye adsorbed (mg g^{-1}) at various times t, q_e is the maximum adsorption capacity (mg g^{-1}) for pseudo-first-order adsorption, k_1 is the pseudo-first-order rate constant for the adsorption process (min^{-1}), q_2 is the maximum adsorption capacity (mg g^{-1}) for the pseudo-second-order adsorption, k_2 is the rate constant of pseudo-second-

Table 1
Langmuir and Freundlich parameters for the adsorption of azocoumarin dye onto ACRS

	Langmuir isotherm			Freundlich isotherm		
Temperature (°C)	q_{max} (mg g^{-1})	K_L (L mg^{-1})	r_L^2	K_F (mg g^{-1})	n	r_F^2
25	69.17	0.0196	0.816	1.652	1.751	0.981
40	84.6671	0.0271	0.889	1.718	1.562	0.986
50	139.56	0.0282	0.902	1.902	1.437	0.994
60	158.544	0.0305	0.954	2.154	1.284	0.999

order adsorption (g mg^{-1} min^{-1}). The straight-line plots of $\log(q_e - q_t)$ vs. t for the pseudo-first-order reaction and t/q_t vs. t for the pseudo-second-order reaction (Figs. 10 and 11) for the adsorption of tested dye onto (ACRS) have also been tested to obtain the rate parameters. The k_1, k_2, q_e, q_2, and correlation coefficients, r_1^2 and r_2^2 for the dye under different temperatures were calculated from these plots and are given in Table 2. The correlation coefficients (r_1^2) for the pseudo-first-order kinetic model are between 0.969 and 0.988 and the correlation coefficients (r_2^2), for the pseudo-second-order kinetic model are between 0.997 and 0.999. It is probable, therefore, that this adsorption system is not a pseudo-first-order reaction, as it fits the pseudo-second-order kinetic model.

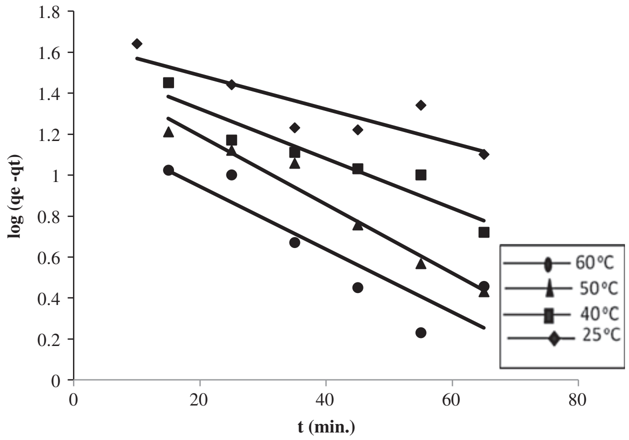

Fig. 10. Pseudo-first-order kinetic plot for the adsorption at different temperatures.

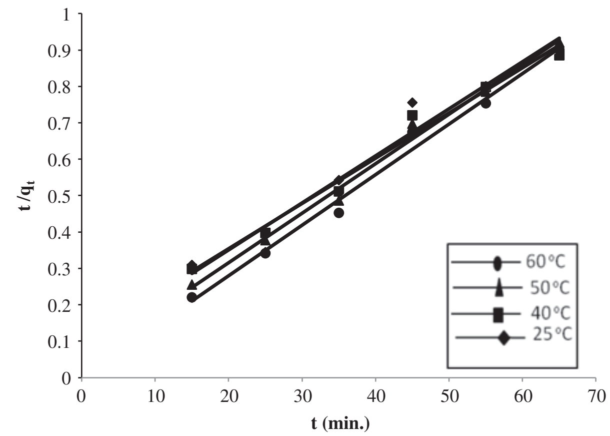

Fig. 11. Pseudo-second-order kinetic plot for the adsorption at different temperatures.

3.10. Thermodynamic parameters

In any adsorption process, both energy and entropy considerations must be taken into account in order to determine what process will occur spontaneously. Values of thermodynamic parameters are the actual indicators for practical application of a process. The amount of the dye adsorbed onto (ACRS) at

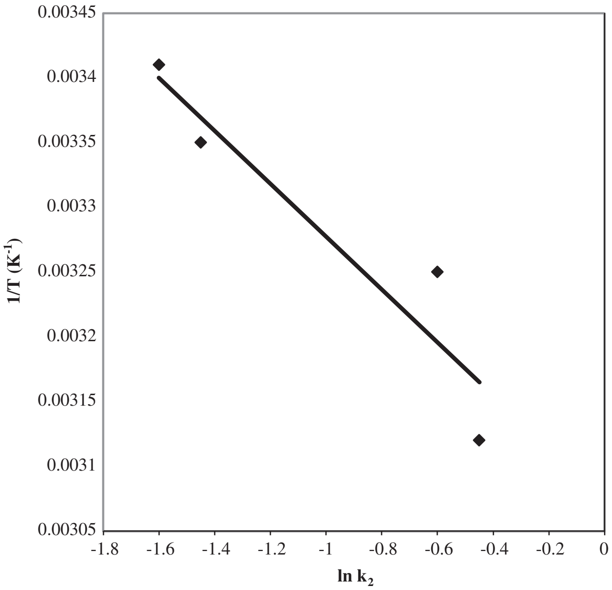

Fig. 12. Arrhenius plot of the adsorption of azocoumarin dye onto ACRS.

Table 2
Pseudo-first-order and pseudo-second-order for the adsorption of azocoumarin dye onto ACRS

	Pseudo-first-order			Pseudo-second-order		
Temperature (°C)	q_e (mg g^{-1})	k_1 (min^{-1})	r_1^2	q_2 (mg g^{-1})	k_2 (g mg^{-1} min^{-1})	r_2^2
25	0.923	3.89	0.969	151.94	0.175	0.997
40	0.934	3.39	0.972	150.37	0.209	0.998
50	0.942	2.98	0.980	150.01	0.479	0.998
60	0.949	2.42	0.988	150.09	0.559	0.999

Table 3
Thermodynamic parameters calculated with the pseudo-second rate constant for azocoumarin onto ACRS

Temperature (°C)	K_C	E_a (kJ mol^{-1})	ΔG° (kJ mol^{-1})	ΔH° (kJ mol^{-1})	ΔS° (J mol^{-1} K^{-1})
25	93.643	12.96	−33.214	−11.83	0.087
40	133.07		−33.625		
50	228.33		−33.972		
60	213.30		−34.113		

equilibrium and at different temperatures 25, 40, 50, 60°C, has been examined to obtain thermodynamic parameters for the adsorption system. The pseudo-second-order rate constant of tested dye adsorption is expressed as a function of temperature by the following Arrhenius type relationship [35]:

$$\ln k_2 = \ln A - E_a/RT \qquad (9)$$

where E_a is the Arrhenius activation energy of adsorption, A is the Arrhenius factor, R is the gas constant and is equal to 8.314 J mol^{-1} K^{-1} and T is the operated temperature. A linear plot of $\ln k_2$ vs. $1/T$ for the adsorption (Fig. 12) was constructed to generate the activation energy from the slope ($-E_a/R$). The chemical (chemisorption) or physical (physisorption) adsorption mechanism are often an important indicator to describe the type of interactions between tested dye and (ACRS). The magnitude of activation energy gives an idea about the type of adsorption which is mainly physical or chemical. Low activation energies (5–40 kJ mol^{-1}) are characteristics for physisorption, while higher activation energies (40–800 kJ mol^{-1}) suggest chemisorption [36]. The result obtained is +12.96 kJ mol^{-1} (Table 3) for the adsorption of the dye onto (ACRS), indicating that the adsorption has a low potential barrier and corresponding to a physisorption.

The other thermodynamic parameters, change in the standard free energy (ΔG°), enthalpy (ΔH°), and entropy (ΔS°) were determined by using following equations:

$$K_C = C_A/C_S \qquad (10)$$

$$\Delta G^\circ = -RT \ln K_C \qquad (11)$$

$$\ln K_C = \Delta S^\circ/R - \Delta H^\circ/RT \qquad (12)$$

where K_C is the equilibrium constant, C_A is the amount of dye adsorbed on the (ACRS) of the solution at equilibrium (mol L^{-1}), and C_S is the equilibrium concentration of the dye in the solution (mol L^{-1}). The q_2 of the pseudo-second-order model in Table 3 was used to obtain C_A and C_S. T is the solution temperature (K) and R is the gas constant. ΔH° and ΔS° were calculated from the slope and the intercept of Van't Hoff plots of $\ln K_C$ vs. $1/T$ (Fig. 13). The results are given in Table 3.

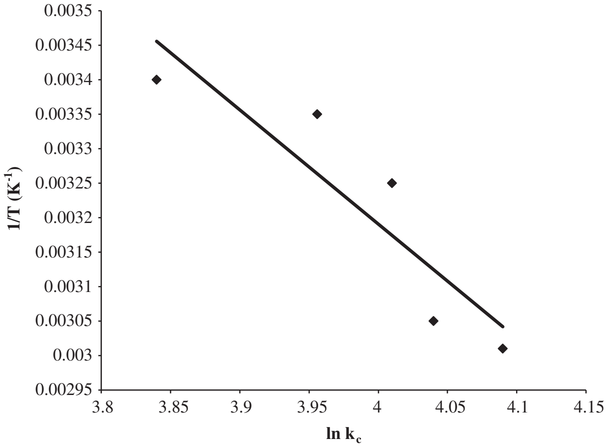

Fig. 13. Van't Hoff plot for determination of thermodynamic parameters for the adsorption.

The values of adsorption thermodynamic parameters are listed in Table 3. The negative value of the change of free energy (ΔG°) confirms the feasibility of the adsorption process and also indicates spontaneous adsorption of tested dye onto (ACRS) in the temperature range studied [37]. The small negative value of the standard enthalpy change (ΔH°) which is (−11.83 kJ mol^{-1}) indicates that the adsorption is physical in nature involving weak forces of attraction and is also exothermic, thereby demonstrating that the process is stable energetically. The low positive value of ΔS° (0.087 J mol^{-1} K^{-1}) suggests the increased randomness of the solid–solution interface during the adsorption of azocoumarin in aqueous solution on ACRS.

4. Conclusion

The present study clearly demonstrated that activated carbon made from rice straw (ACRS) is an effective adsorbent for the removal of azocoumarin from an aqueous solution. The BET surface area and BJH pore volume were calculated and found to be $67.4\ \mathrm{m^2\,g^{-1}}$ and $0.134\ \mathrm{cm^3\,g^{-1}}$, respectively. SEM images show well defined and characterized morphological images that are evident for the effective adsorption of azocoumarin molecules on the cavities and pores of the (ACRS). For the application of Langmuir and Freundlich equations, the experimental results show that the Freundlich model was the best. The highest value of n at equilibrium is 1.75, suggesting that the adsorption is physical. The kinetic data tend to fit very well in the pseudo-second-order kinetics model with high correlation coefficients. The ΔG° values were negative, therefore the adsorption was spontaneous in nature. The negative value of ΔH° reveals that the adsorption process was exothermic in nature. The positive value of ΔS° implies the increment of an orderliness between the adsorbate and the adsorbent molecules.

References

[1] İ. Özbay, U. Özdemir, B. Özbay, S. Veli, Kinetic, thermodynamic and equilibrium studies for adsorption of azo reactive dye onto a novel waste adsorbent: Charcoal ash, Desalin. Water Treat. 51 (2013) 6091–6100.

[2] J. Fu, Z. Chen, M. Wang, S. Liu, J. Zhang, J. Zhang, R. Han, Q. Xu, Adsorption of methylene blue by a high-efficiency adsorbent (polydopamine microspheres): Kinetics, isotherm, thermodynamics and mechanism analysis, Chem. Eng. J. 259 (2015) 53–61.

[3] T. Ma, P.R. Chang, P. Zheng, F. Zhao, X. Ma, Fabrication of ultra-light graphene-based gels and their adsorption of methylene blue, Chem. Eng. J. 240 (2014) 595–600.

[4] S. Sadaf, H.N. Bhatti, Removal of COD from real textile effluents using agro-industrial wastes, Desalin. Water Treat. 53(10) (2015) 2585–2592.

[5] T.A. Ammar, K.Y. Abid, A.A. El-Bindary, A.Z. El-Sonbati, Chlorine dioxide bulk decay prediction in desalinated drinking water, Desalination 352 (2014) 45–51.

[6] R.O. Kennedy, R.D. Thornes, Coumarins: Biology, Applications and Mode of Action, John Wiley and Sons, Chichester, UK, 1997.

[7] S. Noreen, H.N. Bhatti, Fitting of equilibrium and kinetic data for the removal of Novacron Orange P-2R by sugarcane bagasse, J. Ind. Eng. Chem. 20(4) (2014) 1684–1692.

[8] S. Sadaf, H.N. Bhatti, S. Nausheen, S. Noreen, Potential use of low-cost lignocellulosic Waste for the removal of direct violet 51 from aqueous solution: Equilibrium and breakthrough studies, Arch. Environ. Contam. Toxicol. 66(4) (2014) 557–571.

[9] S. Sadaf, H.N. Bhatti, S. Nausheen, M. Amin, Application of a novel lignocellulosic biomaterial for the removal of Direct Yellow 50 dye from aqueous solution: Batch and column study, J. Taiwan Inst. Chem. Eng. 47 (2015) 160–170.

[10] S.S. Madaeni, Z. Jamali, N. Islami, Highly efficient and selective transport of methylene blue through a bulk liquid membrane containing Cyanex 301 as carrier, Sep. Purif. Technol. 81 (2011) 116–123.

[11] N. Serpone, S. Horikoshi, A.V. Emeline, Microwaves in advanced oxidation processes for environmental applications. A brief review, J. Photochem. Photobiol., C 11 (2010) 114–131.

[12] S. Noreen, H.N. Bhatti, S. Nausheen, S. Sadaf, M. Ashfaq, Batch and fixed bed adsorption study for the removal of Drimarine Black CL-B dye from aqueous solution using a lignocellulosic waste: A cost affective adsorbent, Ind. Crops Prod. 50 (2013) 568–579.

[13] X. Jiang, Y. Sun, L. Liu, S. Wang, X. Tian, Adsorption of C.I. Reactive Blue 19 from aqueous solutions by porous particles of the grafted chitosan, Chem. Eng. J. 235 (2014) 151–157.

[14] F. Güzel, H. Sayğılı, G.A. Sayğılı, F. Koyuncu, Elimination of anionic dye by using nanoporous carbon prepared from an industrial biowaste, J. Mol. Liq. 194 (2014) 130–140.

[15] A.A. El-Bindary, A.Z. El-Sonbati, A.A. Al-Sarawy, K.S. Mohamed, M.A. Farid, Adsorption of hazardous azocoumarin from aqueous solution using activated carbon made from rice straw, J. Mater. Environ. Sci. 6 (2015) 1–10.

[16] A.A. El-Bindary, M.A. Diab, M.A. Hussien, A.Z. El-Sonbati, A.M. Eessa, Adsorption of Acid Red 57 from aqueous solutions onto polyacrylonitrile/activated carbon composite, Spectrochim. Acta Part A Mol. Biomol. Spectrosc. 124 (2014) 70–77.

[17] A.A. El-Bindary, M.A. Hussien, M.A. Diab, A.M. Eessa, Adsorption of Acid Yellow 99 by polyacrylonitrile/activated carbon composite: Kinetics, thermodynamics and isotherm studies, J. Mol. Liq. 197 (2014) 236–242.

[18] A.A. El-Bindary, A.Z. El-Sonbati, A.A. Al-Sarawy, K.S. Mohamed, M.A. Farid, Adsorption and thermodynamic studies of hazardous azocoumarin dye from an aqueous solution onto low cost rice straw based carbons, J. Mol. Liq. 199 (2014) 71–78.

[19] I.D. Mall, V.C. Srivastava, G.V.A. Kumar, I.M. Mishra, Characterization and utilization of mesoporous fertilizer plant waste carbon for adsorptive removal of dyes from aqueous solution, Colloids Surf., A 278 (2006) 175–187.

[20] K.Y. Foo, B.H. Hameed, Insights into the modeling of adsorption isotherm systems, Chem. Eng. J. 156 (2010) 2–10.

[21] S. Brunauer, P.H. Emmett, E. Teller, Adsorption of gases in multimolecular layers, J. Am. Chem. Soc. 60 (1938) 309–319.

[22] S. Sadaf, H.N. Bhatti, M. Arif, M. Amin, F. Nazar, Adsorptive removal of direct dyes by PEI-treated peanut husk biomass: Box–Behnken experimental design, Chem. Ecol. 31 (2015) 252–264.

[23] M.R. Khan, M. Ray, A.K. Guha, Mechanistic studies on the binding of Acid Yellow 99 on coir pith, Bioresour. Technol. 102 (2011) 2394–2399.

[24] R. Ahmad, R. Kumar, Adsorption studies of hazardous malachite green onto treated ginger waste, J. Environ. Manage. 91 (2010) 1032–1038.

[25] H.R. Guendy, Treatment and reuse of wastewater in the textile industry by means of coagulation and

adsorption techniques, J. Appl. Sci. Res. 6(8) (2010) 964–972.

[26] I. Langmuir, The constitution and fundamental properties of solids and liquids. I. Solids, J. Am. Chem. Soc. 38 (1916) 31–60.

[27] I. Langmuir, The constitution and fundamental properties of solids and liquids. II. Liquids, J. Am. Chem. Soc. 39 (1917) 1848–1906.

[28] I. Langmuir, The adsorption of gases on plane surfaces of glass, mica and platinum, J. Am. Chem. Soc. 40 (1918) 1361–1403.

[29] A.R. Alley, Water Quality Control Handbook, McGraw-Hill Education, Europe, London, 2000, pp. 125–141.

[30] H.M.F. Freundlich, Uber die adsorption in lasugen (Over the adsorption in solution), Z. Phys. Chem. (Leipzig) 57A (1906) 385–470.

[31] S. Tunali, A.S. Ozcan, A. Ozcan, T. Gedikbey, Kinetics and equilibrium studies for the adsorption of Acid Red 57 from aqueous solutions onto calcined-alunite, J. Hazard. Mater. 135 (2006) 141–148.

[32] J.-O. Jiang, C. Cooper, S. Ouki, Comparison of modified montmorillonite adsorbents, Chemosphere 47 (2002) 711–716.

[33] S. Lagergren, Zurtheorie der sogenannten adsorption gelosterstoffe (About the theory of so-called adsorption of soluble substances), Kungliga Svenska Vetenskapsakademiens, Handlingar 24(4) (1898) 1–39.

[34] Y.S. Ho, G. McKay, Sorption of dye from aqueous solution by peat, Chem. Eng. J. 70(2) (1998) 115–124.

[35] R.S. Juang, F.C. Wu, R.L. Tseng, The ability of activated clay for the adsorption of dyes from aqueous solutions, Environ. Technol. 18(5) (1997) 525–531.

[36] H. Nollet, M. Roels, P. Lutgen, P. Van der Meeren, W. Verstraete, Removal of PCBs from wastewater using fly ash, Chemosphere 53(6) (2003) 655–665.

[37] M.J. Jaycock, G.D. Parfitt, Chemistry of Interfaces, Ellis Horwood Ltd, Onichester, 1981.